



# Lines and dots: characteristics of the motion integration process

Ivan Lamouret \*, Valérie Cornilleau-Pérès, Jacques Droulez

*Laboratoire de Physiologie de la Perception et de l'Action, CNRS-Collège de France, 11, place Marcelin Berthelot, 75 005 Paris, France*

Received 7 July 2000

## Abstract

Local motion detectors can only provide the velocity component perpendicular to a moving line that crosses their receptive field, leading to an ambiguity known as the 'aperture problem'. This problem is solved exactly for rigid objects translating in the screen plane via the intersection of constraints (IOC). In natural scenes, however, object motions are not restricted to fronto-parallel translations, and several objects with distinct motions may be present in the visual space. Under these conditions the usual IOC construction is no longer valid, which raises questions as its use as a basis for spatial integration and selection of motion signals in uniform and non-uniform velocity fields. The influence of the motion of random dots on the perceived direction of a horizontal line grating was measured, when dots and lines are seen through different apertures. The random dots were mapped on a plane that translates in a fronto-parallel plane (uniform 2D translation) or in depth (3D, corresponding to a non-uniform projected velocity field, either expanding or contracting). The grating was either moving rigidly with the dots or in the opposite direction. Subjects' responses show that the direction of line grating movement was reliably influenced only in conditions consistent with rigid motion; where there was a reliable influence, the perceived direction was consistent with the dot motion pattern. This finding points to the existence of a motion-based selection mechanism that operates prior to the disambiguation of the line movement direction. Disambiguation could occur for both uniform and non-uniform velocity fields, even though in the last case none of the individual dots indicated the proper direction in 2D velocity space. Finally, the capture by non-uniform motion patterns was less robust than that by uniform 2D translations, and could be disrupted by manipulations of the shape and size of the apertures. © 2001 Elsevier Science Ltd. All rights reserved.

*Keywords:* Motion perception; Aperture problem; Perceptual grouping; Segmentation; Three-dimensional motion

## 1. Introduction

A common understanding of visual motion perception follows the general framework proposed by Marr (1982) to describe visual perception, that decomposes visual processes into several steps, from spatial and temporal retinal inputs to object representation. Schematically, in the first step, motion is detected in the direction of the strongest variation of image luminance (Marr & Ullman, 1981; Van Santen & Sperling, 1984; Adelson & Bergen, 1985). Local motion detectors only specify the velocity component parallel to the luminance gradient. In a second step, the complete retinal velocity field is recovered by using additional assumptions about the underlying visual scene. The question of determining these assumptions is known as the 'aper-

ture problem'. It is usually solved by looking for a smooth bi-dimensional (2D) velocity field (Horn & Schunck, 1981; Adelson & Movshon, 1982; Hildreth, 1984; Yuille & Grzywacz, 1988). Finally, in the third step, the three-dimensional (3D) motion is extracted (Longuet-Higgins & Prazdny, 1980; Koenderink & van Doorn, 1987; Perrone & Stone, 1994).

This decomposition has received neurophysiological support with the possible identification of each step with a visual cortical area in the macaque monkey. Hubel and Wiesel (1968) found cells in area V1, which were selective for the direction of line movement. To distinguish between the first and second steps, Movshon, Adelson, Gizzi, and Newsome (1985) used plaid stimuli composed of two superimposed sinusoidal gratings of different orientations. In area MT they found two types of direction selective neurons, one being only sensitive to the movement of the component gratings (component motion), the other being sensitive

\* Corresponding author.

E-mail address: ivan.lamouret@college-de-france.fr (I. Lamouret).

to the movement of the plaid (pattern motion). By contrast in V1 they identified only neurons of the first type. Since MT receives strong feed-forward inputs from V1, Movshon et al. concluded that MT might be the locus for the processing of 2D velocity from 1D motion signals. Further in the dorsal visual pathway that goes from V1 to the posterior parietal cortex, in area MST, several groups identified neurons that were specifically sensitive to spatial variations of image velocity (contraction, rotation, rotation in depth) and could therefore account for a process of 3D analysis of optic flow (Saito, Yukie, Tanaka, Hikosaka, Fukuda, & Iwai, 1986; Tanaka, Sugita, Moriya, & Saito, 1993; Duffy & Wurtz, 1991a,b; Lagae, Maes, Raiguel, Xiao, & Orban, 1994). Such selective neurons were not found in area MT (Lagae et al., 1994). In addition to the functional similarity of these areas to the different steps described above, the fact that they are strongly connected to each other, with feed-forward connections following the hierarchic order of the cortex anatomical organization (Maunsell & Van Essen, 1983; Felleman & Van Essen, 1991) is another argument for this decomposition.

Psychophysical studies have usually addressed these different steps separately. As far as the second step (computation of the retinal velocity field) is concerned, most studies have only used uniform motion (fronto-parallel translation). Plaids have been widely used for studying the aperture problem. Adelson and Movshon (1982) described the geometrical construction of a plaid velocity from the velocity of its grating components. The set of possible velocities of a single grating defines a line in velocity space (constraint line). The only velocity compatible with the rigid translation of the plaid is therefore the intersection of constraints (IOC). When the two component gratings are similar in contrast, spatial frequency and velocity, the IOC model closely predicts the perceived velocity of the pattern. However, when the two grating components are too dissimilar there is a significant bias in perceived direction (Stone, Watson, & Mulligan, 1990; Kooi, De Valois, Grosf, & De Valois 1992; Burke & Wenderoth, 1993). Yo and Wilson (1992) used plaids of similar contrasts and spatial frequencies but of different velocities. They found that the perceived movement is initially in the direction of the vector average of component velocities, but shifts progressively, when stimulus duration increases, towards the direction predicted by the IOC model. However, plaids may not be appropriate stimuli for studying the aperture problem since it has been argued that second order ('blobs', Gorea & Lorenceau, 1991) and non-Fourier (Wilson, Ferrera, & Yo, 1992) processing can unambiguously define the pattern velocity.

Several groups have discussed the influence of terminations, dots or blobs on the perceived motion of lines.

The perceived rigidity of a moving curved line is increased when either terminations are added to the line, or moving dots are added in the vicinity of the incurvation (Nakayama & Silverman, 1988). Also, the 'barber pole effect' is a classical demonstration of the influence of the distribution of line terminators on the perceived velocity of the lines: when seen behind an invisible rectangular aperture, a moving grating appears to move in the direction of the aperture side that contains the greatest number of line endings (Wallach, 1935, 1976). Shiffrar, Li, and Lorenceau (1995) have shown that dots presented between the lines of a barber pole stimulus can modify the perceived motion direction. Increasing the proportion of dots relative to the number of influential line terminators shifts the perceived motion direction of the lines toward the motion direction of the dots. However, the presence of dots or line terminations moving coherently with lines is not a prerequisite to the resolution of the aperture problem. For instance, Lorenceau and Shiffrar (1992) described conditions in which one can perceive the correct movement of a square when all the square corners are hidden. This demonstrated that ambiguous velocity measurements can be spatially integrated to solve the aperture problem.

### *1.1. The aperture problem: beyond translation in the screen plane of a single object*

In the authors' view previous psychophysical studies of the aperture problem present two major limitations: in natural scenes, motion is not restricted to fronto-parallel translation, and several objects with different motions may be present. In these conditions, the usual construction of IOC is no longer valid, except for velocity signals extracted at the same retinal location. Here these two limitations are reviewed as well as related aspects of computational approaches.

A first limitation of the experiments described above is that they consider only spatially uniform motion, although in general the projected velocity field of 3D object motion is non-uniform. To handle motion integration in complex flows, several computational models propose to compute the smoothest velocity field consistent with local velocity measurements, rather than a uniform one. These schemes usually minimize the spatial variations of the 2D velocity vector field (Horn & Schunck, 1981; Hildreth, 1984), although the smoothing procedure can be directly applied to 3D velocity retinal fields (Scott, 1986; Tziritas, 1987; Droulez & Cornilleau-Pérès, 1993). The advantage of the latter scheme lies in its geometrical interpretation in 3D space: indeed, the visual scene under analysis is supposed to be locally planar and rigid (Droulez & Cornilleau-Pérès, 1993). From a computational point of view, this method turns out to produce a very accurate retinal

velocity field when applied to synthetic images, thus allowing a better computation of 3D object motion at later stages (Scott, 1986). The computation of parametric flow fields has also been proposed (e.g. affine, Bouthemy & Santillana-Rivero, 1987) that bypasses the computation of the 2D velocity at each point, and extracts directly spatio-temporal derivatives of the velocity field. However, in contrast to smoothing schemes, these approaches do not explicitly tackle the problem of disambiguating local velocity measurements, because they do not directly provide local velocity estimates. Of course they can be adapted to do so and extrapolate local velocities from the computed parametric velocity field. Hence the question arises whether and how the integration process involved in the perception of motion operates for non-uniform movement, and whether it involves a 3D or a parametric representation of retinal motion.

Mingolla, Todd, and Norman (1992) studied the ability to integrate line motion across multiple apertures for uniform (translation) and non-uniform (rotation + expansion or contraction) velocity fields. They found that, in the absence of visible line intersections and line endings, discrimination between the expansion and contraction components of the rotating line texture was totally biased by the orientation sampling of the texture. When there was no bias in the orientation sampling, subjects could not discriminate between expansion and contraction. However, in the same experimental conditions the perception of 2D translations was just as biased by the orientation sampling of the texture, and in the absence of orientation bias, discrimination performance was also poor. These results are consistent with the idea that discrimination of translations and expansions involves similar mechanisms, and the authors proposed that in both cases a local averaging of line velocities preceded the identification of the motion pattern. However, Lorenceau and Shiffrar (1992) have shown that motion integration across apertures is sensitive to stimulus parameters such as line contrast, with better discrimination performance at low contrast. It is believed that motion integration in complex flow fields should be studied in experimental conditions that favor integration even for 2D translation (a particular case of 3D motion).

A second point that has scarcely been addressed concerns the need for coherence of the velocity signals to be integrated. Indeed, when several objects have distinct movements in the visual scene, combining all measurements would lead to false velocity estimates. This problem was noticed by Marr and Ullman (1981), and Hildreth (1984), who proposed to stop the integration process along contours whenever two ambiguous velocity measurements are not compatible; unfortunately this occurs only for contours of identical orientations and different normal velocity components.

Although for two ambiguous signals of different orientations there is always a rigid translation defined by the IOC, this is not true whenever the image contains more than two orientations: Schunck (1986) proposed to use a voting scheme to select the tightest cluster of IOC constructed from local velocity measurements in a small patch of the image. More recently Nowlan and Sejnowski (1995) constructed a neural network that builds an explicit representation of the reliability of the velocity estimate over a patch of the image (which is related to the orientation content in the patch). Velocities are then selectively extracted from the most reliable parts of the image, thus allowing the detection of several global motions in the same image. But this model only deals with uniform 2D motion, and does not address the problem of disambiguating motion signals in the least reliable parts of the image.

Most psychophysical studies of the aperture problem have used stimuli compatible with a single rigid translation. For example in all the experiments described above that studied the effect of moving dots on the perceived movement of lines, dots and lines always had equal velocity components in the direction normal to the line. van den Berg and van de Grind (1993) added texture to moving plaids in order to disambiguate one of the component velocities. These authors observed that when the texture motion is not compatible with the second grating the plaid does not cohere, two transparent gratings with different motions are being perceived instead. However, this study was restricted to translational motion, and to spatially superimposed signals. Another question arises, therefore, as to whether motion integration still operates when velocity signals in a neighborhood are not ambiguous, and define a motion pattern (possibly non uniform) that is not compatible with the constraint line of the ambiguous signal.

Hence the goal of the present experiments is to explore the following questions. (1) Are ambiguous and unambiguous velocity signals spatially integrated in case of non-uniform motion? (2) Is this integration process linear relative to the unknown velocity component or does it rely on a selection process that tests the consistency between ambiguous and unambiguous velocity measurements? (3) What kind of unambiguous signals are involved in the selection and integration processes?

Part of this work has been reported in abstract form (Lamouret, Cornilleau-Péres, & Droulez, 1995).

## 2. Methods

### 2.1. Rationale

In two experiments the influence of a random dot velocity field on the perceived velocity of a horizontal

line grating was tested. The dots and lines were presented in separate apertures, in order to eliminate local

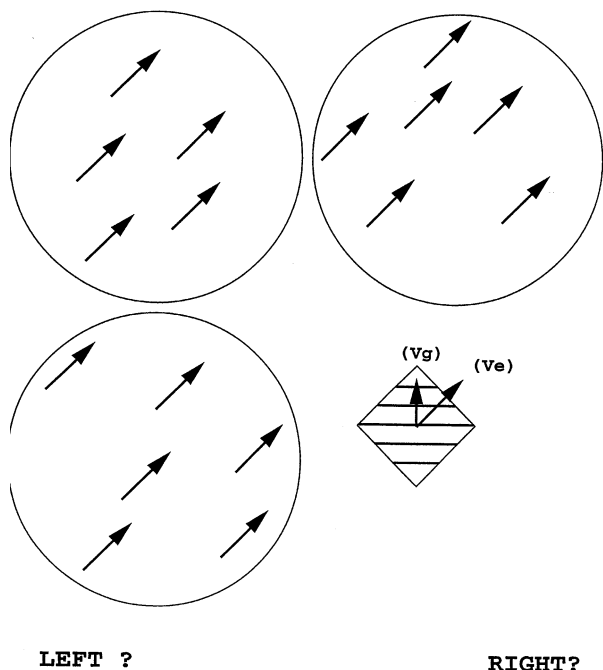


Fig. 1. Stimulus in the *Coherent 2D* condition. Behind each circular aperture, random dots are undergoing translation in a diagonal direction ( $V_e$ ), their vertical velocity component is equal to the grating normal velocity ( $V_g$ ). The subject's task is to indicate the direction of the perceived horizontal component of the grating velocity. In the actual display the occluding mask was black, the background was grey and the dots and lines were white (see text).

effects and assess the role of the motion pattern of the dots (either a uniform flow corresponding to a fronto-parallel translation, referred as *2D* (Fig. 1), or a contraction or expansion flow centered on the middle of the screen (Fig. 2), corresponding to a translation in depth, referred as *3D*). For a given dot motion pattern, we define the *extrapolated velocity* as the velocity extrapolated from the pattern at the image locus of the grating. The influence of consistency was evaluated by setting the grating velocity equal (*coherent*) or opposite (*incoherent*) to the vertical component of the *extrapolated velocity*. For each motion pattern, the *extrapolated velocity* could have a horizontal component directed to the right or to the left. In a two-alternative forced choice procedure (2AFC), subjects were asked to indicate the direction (left or right) of the perceived horizontal velocity component of the line grating. In addition, a control condition consisted in a motionless random dot pattern, with the grating moving as in the other conditions, referred to as *NoDotMotion*. For this condition, the *extrapolated velocity* was arbitrarily defined as directed towards or away from the screen center, in order to obtain the same symmetries of response categories as in the other conditions, and to quantify response biases in the experimental set-up.

The eccentricity and size of the grating were chosen so that, in our conditions of contraction and expansion, the variations of line motion with eccentricity were smaller than what could be displayed between two frames with the pixel resolution of the screen. Therefore, up to the screen resolution, the grating motion is compatible with the expansion or contraction velocity field, and due to screen aliasing it is uniform throughout the aperture. In this way, the grating motion was strictly identical in the conditions of 2D translation and expansion/contraction, while for each condition it is compatible with the motion pattern of the dots.

## 2.2. Apparatus and stimuli

Stimuli were displayed on the SONY monitor of a Silicon Graphics Indy workstation (refresh rate: 72 Hz, resolution:  $1280 \times 1024$  pixels). They consisted of four apertures of different shapes, each located in one quadrant of the screen, and containing lines or dots in motion. The aperture containing the horizontal line grating, which had the shape of a diamond, was  $2.3^\circ$  in its diagonal. It was located at  $4.4^\circ$  from the center of the screen, and was presented randomly in four different positions (one in each of the four quadrants). The three other apertures, located in the three remaining quadrants, contained the moving dots. In the first experiment they were all circular (Figs. 1 and 2). In the second experiment two of them were semi-circular and the three of them lay on the same side of a screen

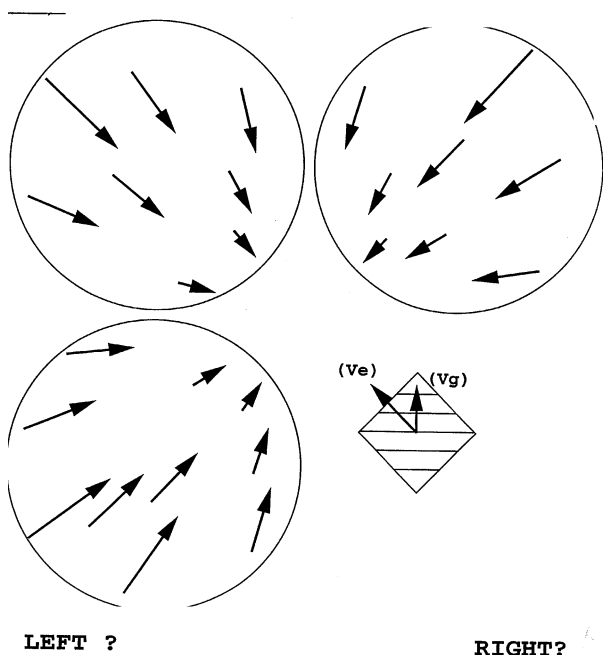


Fig. 2. Stimulus in the *Coherent 3D* condition. The contracting velocity field is simulating a translation in depth. The *extrapolated velocity* ( $V_e$ ) is directed at the center of the display, its vertical component is equal to the grating normal velocity ( $V_g$ ).

diagonal (Fig. 5). They were presented at  $6.9^\circ$  from the center of the screen, and were  $9.8^\circ$  in diameter. The whole pattern covered  $20^\circ \times 20^\circ$  of the visual field. The luminance of the dots and lines was  $3.8 \text{ cd/m}^2$ , the luminance of the background was  $1.3 \text{ cd/m}^2$ , and the occluding mask was black.

Within the diamond-shaped aperture, the grating moved vertically, and its movement was directed upwards or downwards with equal probability. The lines were one pixel wide, and their vertical velocity was  $1.4^\circ/\text{s}$  (one pixel per frame). The dots (one pixel) were displayed in the three other apertures with uniform dot density (about 5 dots/ $^\circ^2$ , corresponding to 1200 dots in experiment 1, and 800 dots in experiment 2). Translations were directed along the diagonals. In the translation condition the dot speed was  $2^\circ/\text{s}$  and in the expansion and contraction conditions it increased linearly with eccentricity from  $1.3^\circ/\text{s}$  at  $2.9^\circ$  of eccentricity to  $5.3^\circ/\text{s}$  at  $11.8^\circ$  of eccentricity (the focus of expansion was not visible). Thus the grating vertical velocity was always equal to the vertical component of the dot velocity at  $4.4^\circ$  of eccentricity on the diagonals. Movement duration was 160 ms in order to minimize eye movement during trials. Stimuli were presented motionless during 1 s before and after the movement.

### 2.3. Subjects

Three subjects participated to the first experiment and three others to the second experiment. All were between 20 and 31 years old, and had normal (uncorrected) vision. They were naive paid volunteers, and gave their informed and written consent. None of them had previously participated in a psychophysical experiment.

### 2.4. Procedure

Viewing was monocular to avoid conflicting stereoscopic cues in the case of translation in depth.

The head was maintained at 80 cm from the screen by a chinrest. Both eyes were successively tested in the first experiment, while only the right (dominant) eye was tested in the second experiment.

Subjects completed 18 blocks of trials, in which all conditions were presented in random order. Each block comprised 40 trials in the first experiment, and 56 trials in the second experiment (i.e. 4 positions of the diamond  $\times$  5 or 7 different patterns of the dot movement  $\times$  2 horizontal directions of the *extrapolated velocity*). The total duration of the experiment was one hour for each eye in the first experiment, and one-hour-and-a-half in the second one, not taking into account regular pauses in daylight.

One second before each stimulus presentation, a red fixation cross was placed in the center of the diamond-

shaped aperture that was to appear next. The fixation cross was maintained during the 1 s stimulus onset, and was removed during the movement. Subjects were asked to fixate the red cross, and to report with the mouse keys the direction of the grating movement in the horizontal direction (left or right). The fixation cross reappeared in a new position immediately after the subjects responded.

The experimental room was dark. After 5 min of adaptation to darkness, subjects were trained with a dozen stimuli in order to make sure that they had understood the task, and began the experiment.

## 3. First experiment

### 3.1. Conditions

The line grating could occupy randomly four different positions (one in each quadrant of the screen), and was seen through a diamond-shaped aperture. The pattern motion of the dots was seen through three circular apertures located in the remaining three quadrants of the screen. The fronto-parallel translation (*2D*) was directed along the screen diagonal that does not intersect with the grating (Fig. 1). The translation in depth (*3D*) resulted in a contraction or expansion flow centered on the middle of the screen (Fig. 2). The *extrapolated velocity* was equal to that of all dots for the uniform *2D* translation conditions. For the *3D* conditions, it corresponds to the *2D* projection of the translation in depth at the image locus of the grating: it is a velocity oriented along the diagonal of the display, directed toward the center of the screen (contraction) or in the opposite direction (expansion). Note that the *extrapolated velocity* in the *3D* translation-in-depth conditions is always directed in the direction opposite to the mean *2D* velocity of the dot velocity field. These two motion patterns, together with the direction of the grating motion, resulted in four conditions, *Coherent 2D*, *Coherent 3D*, *Incoherent 2D*, and *Incoherent 3D*. These four conditions and the *NoDotMotion* condition are shown in Fig. 3 for one particular position of the grating.

### 3.2. Results

Fig. 4 reports the percentages of rightwards responses for the five pattern motion conditions, when the horizontal component of *extrapolated velocity* is directed to the left (open squares) and to the right (filled squares). Responses are averaged over all grating positions, and both eyes. For individual plots, the error bars indicate the confidence intervals computed from the averaged percentages over the four grating positions. Conditions in which the responses are statistically

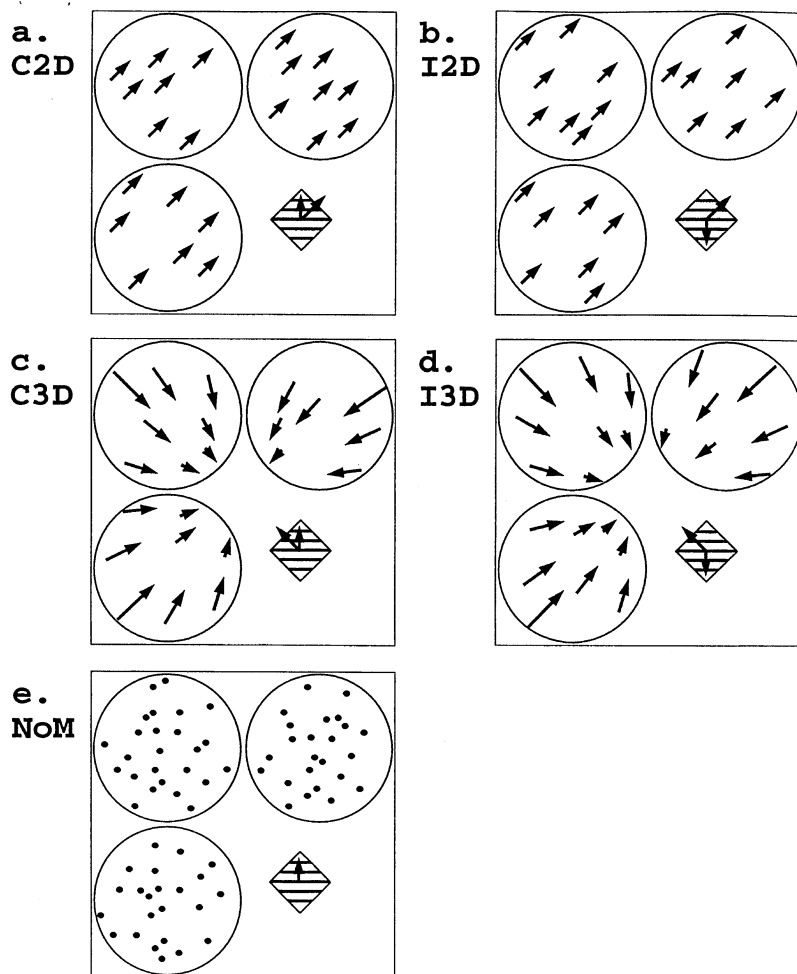


Fig. 3. First experiment conditions, shown with the grating in the lower right quadrant. In the actual experiment the grating was randomly presented in each of the four quadrants. In these examples, for the *Coherent* conditions, the grating is moving upwards, while for the same dot velocity pattern, the grating is moving downwards in the *Incoherent* conditions. In the fifth condition (*NoDotMotion*), the dots are stationary throughout stimulus presentation.

different for rightward and leftward *extrapolated velocity* are marked with an asterisk in the plot of means.

### 3.2.1. Statistical analysis

The effects of the different experimental parameters were assessed with a 4-way ANOVA on the percentage of rightwards responses, corrected with an angular transformation for binomial proportion (Snedecor and Cochran, 1989). The four factors are the pattern motion **condition** (5 levels), the grating **position** (4 levels), the **direction** of the horizontal component of the *extrapolated velocity* (2 levels), and stimulated **eye** (2 levels).

The only statistically significant main effect was found for the **direction** factor ( $F(1,2) = 34.8$ ,  $* P < 0.03$ ). For the **condition** factor ( $F(4,8) = 2.3$ ), the **position** factor ( $F(3,6) = 1.2$ ), and the **eye** factor ( $F(1,2) = 0.08$ ) the main effects were not statistically significant ( $P = 0.15$ ,  $P = 0.39$ ,  $P = 0.94$ , respectively). There were two small interactions, between the **position** and **condition** factors

( $F(12,24) = 2.6$ ,  $P = 0.02$ ) and the **eye**, **direction** and **position** factors ( $F(3,6) = 6$ ,  $P = 0.03$ ), but the most significant interaction was between the **condition** and **direction** factors ( $F(4,8) = 30.9$ ,  $*** P < 0.0001$ ). In other words, the influence of the *extrapolated velocity* depended on the condition. This result was refined by conducting for each condition a contrast analysis between the two levels of the **direction** factor (*extrapolated velocity* to the left or to the right). In the *Coherent* conditions the effects were statistically significant (*Coherent 2D*:  $F(1,2) = 205$ ,  $* P < 0.05$ ; *Coherent 3D*:  $F(1,2) = 11906$ ,  $*** P < 0.0001$ ), whereas in the *Incoherent* and the *NoDotMotion* conditions, they were not (*Incoherent 2D*:  $F(1,2) = 0.86$ ,  $P = 0.45$ ; *Incoherent 3D*:  $F(1,2) = 2.4$ ,  $P = 0.26$ ; *NoDotMotion*:  $F(1,2) = 0.12$ ,  $P = 0.76$ ). Although subjects DH and EA show a small tendency to give responses in the direction opposite to the *extrapolated velocity* in the *Incoherent* conditions, this tendency is not statistically significant for the set of subjects considered here.

Conditions were finally compared to each other by conducting a Least Squares Difference Post-Hoc Test on the differences between right and left scores: for these differences, *Coherent 2D* and *3D* conditions (\*\*  $P < 0.005$ ) were statistically different from the *NoDotMotion* condition, while the *Incoherent 2D* and *Incoherent 3D* conditions were not ( $P = 0.24$ , and  $P =$

0.20, respectively). This confirms that the size of the ‘repulsion’ effect seen in the *Incoherent* conditions could not be distinguished from the response pattern in the ‘control’ condition. Both *Coherent* conditions were statistically different from their *Incoherent* counterpart (\*\*  $P < 0.001$ ), indicating that subjects did not base their responses on the dot velocity pattern only. The *Coherent 2D* condition was statistically different from the *Coherent 3D* condition (\*  $P < 0.01$ ); this shows that the better integration in the *Coherent 2D* condition relative to the *Coherent 3D* condition that can be seen for all subjects is statistically significant.

### 3.2.2. Conclusions

The fact that *Coherent* and *Incoherent* conditions give different results validates the use of these stimuli: had the subjects responded solely on the basis of the moving dots without reference to the grating, their responses would be similar in those conditions. In both *Coherent* conditions (*2D* or *3D*) subjects answer consistently with the movement of the surrounding dots, that is their responses are compatible with the perception of a single rigid object comprising dots and lines, moving behind all apertures. This confirms that the perceived direction of a line grating can be influenced by a surrounding stimulation. For all subjects the effect was stronger in the *Coherent 2D* than in the *Coherent 3D* condition.<sup>1</sup> In the *Incoherent* conditions subjects’ answers were not statistically different when the *extrapolated velocity* had a rightward or leftward horizontal component. Also, they were not statistically different from that in the *NoDotMotion* condition. This shows that the motion integration process is not linear relatively to the unknown component of the grating velocity, but involves a selection process that test the consistency between the motion pattern and the grating motion.

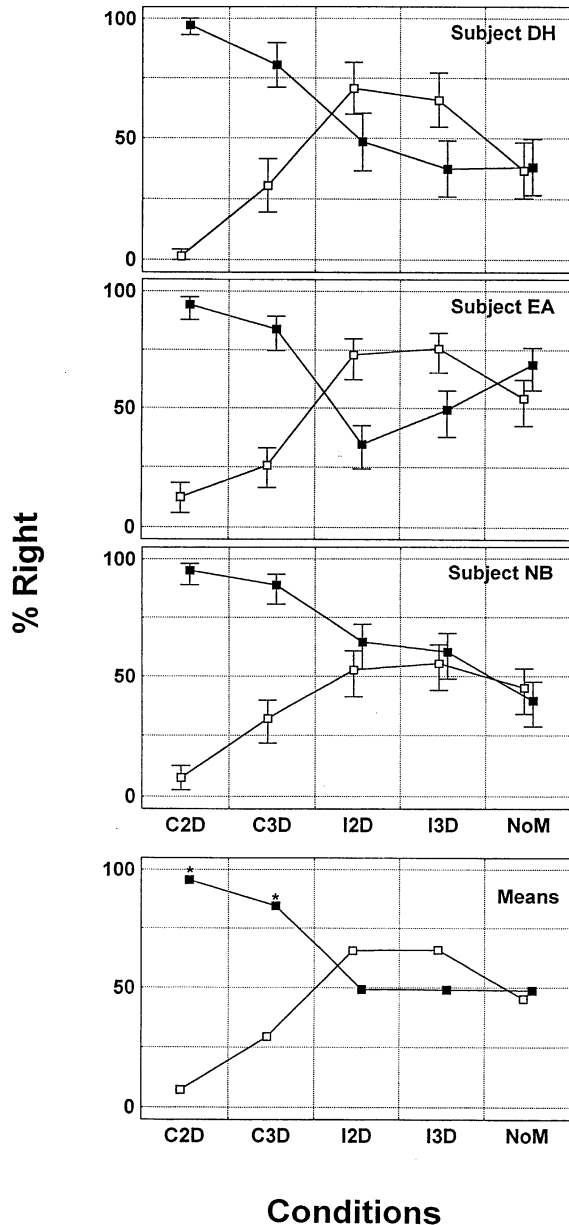


Fig. 4. Results of the first experiment: percentages of rightwards responses for the five pattern-motion conditions, when the horizontal component of the *extrapolated velocity* is leftwards (open squares) and rightwards (filled squares). Responses are averaged over all grating positions, and both eyes. Individual data are plotted with their confidence intervals. For the data averaged over the three subjects, the conditions under which the responses are statistically different for right and left *extrapolated velocity* are marked with an asterisk. Note that the definition of the *extrapolated velocity* in the *NoDotMotion* condition is arbitrary (see the Section 2.1).

## 4. Second experiment

The geometry of the apertures was chosen in such a way that the quadrant that contained the grating did not contain any dot. Because of the relationship between the position of the dots and their velocity for the translation-in-depth motion pattern, the *extrapolated velocity* (at the locus of the grating) could not be estimated from any single dot in the *3D* conditions. However, velocity interpolation between the dots that lie on the grating side of the screen diagonal could be used as a two-dimensional basis for subjects’ responses in the *3D* conditions. Therefore the first experiment does not allow us to discriminate between the *2D* and

<sup>1</sup> In *3D Coherent* condition subjects verbally reported a movement in depth of the grating, and the clear impression that the task was harder when this occurred.

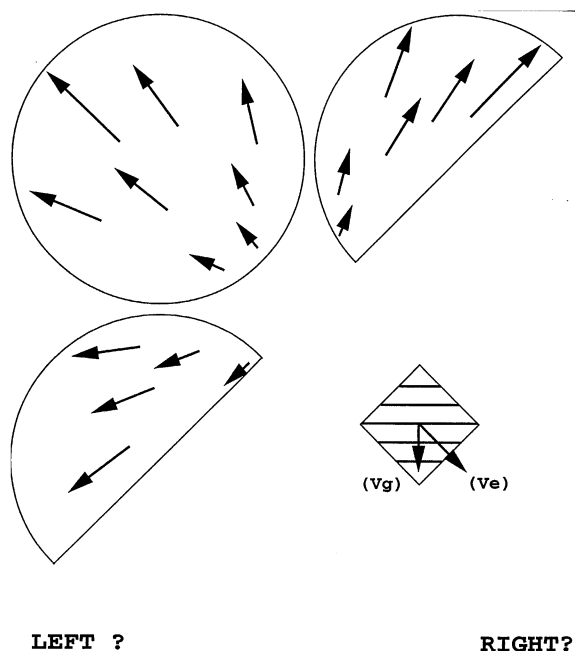


Fig. 5. Outline of the apertures in the second experiment.

3D retinal velocity field hypotheses. In the second experiment we modify the dot apertures so that: (1) no averaging process either global or local, applied on 2D dot velocity, could be correlated with the *extrapolated velocity* in 3D conditions; (2) the three-dimensional velocity field could still be recovered from the dots. Hence the outlines of two circular apertures were replaced by semi-circular apertures in order to suppress the dots that were nearest to the grating (Fig. 5). The number of dots visible behind these apertures was reduced in order to keep the dot density constant.

Another fronto-parallel translation ( $2D'$ ) was also added along the second diagonal. This translation is equal to the mean 2D velocity of 3D motion with this new aperture layout, and strictly opposite to 3D *extrapolated Velocity*. Moreover for this translation, as for 3D motion and in contrast to 2D motion, the *extrapolated velocity* lies on the diagonal containing the grating. This condition was added to have the same relationship between grating direction and the *extrapolated velocity* for one fronto-parallel translation and the 3D motion, which makes the comparisons between the conditions more direct. The corresponding conditions are referred to as *Coherent 2D'* and *Incoherent 2D'*.

In all other respects methods and stimuli were the same as in the first experiment.

All seven conditions for the second experiment are shown in Fig. 6. Since there was no effect of the stimulated eye in the first experiment, the right (dominant) eye was stimulated in this experiment.

#### 4.1. Results

Fig. 7 shows the percentage of rightwards responses when the *extrapolated velocity* was directed leftwards (empty squares) and rightwards (filled squares) in each of the seven conditions for each of the three subjects, and the mean for all three subjects. For individual plots, the error bars indicate the confidence intervals computed from the averaged percentages over the four grating positions. Conditions in which the responses are statistically different for rightward and leftward *extrapolated velocity* are marked with an asterisk in the plot of means.

##### 4.1.1. Statistical analysis

The same data analysis was applied as in the first experiment: a 3-way ANOVA was first performed to assess the effects of the different experimental parameters, this analysis was refined by contrasting the right and left levels of the direction factor for each condition, and Post-Hoc analysis was then conducted to compare conditions.

A 3-way ANOVA was performed on the percentage of rightwards responses corrected with an angular transformation for binomial proportion (Snedecor and Cochran, 1989). The three factors are the pattern motion **condition** (7 levels), the grating **position** (4 levels) and the **direction** of the horizontal component of the *extrapolated velocity* (2 levels, right and left).

There were no statistically significant main effects (**condition**:  $F(6,12) = 1.2$ ,  $P = 0.38$ , **position**  $F(3,6) = 2.14$ ,  $P = 0.2$ , **direction**  $F(1,2) = 14.6$ ,  $P = 0.06$ ). The only statistically significant interaction was between the **condition** and **direction** factors ( $F(6,12) = 17.17$ ,  $*** P < 0.0001$ ). A contrast analysis was then conducted for each condition, between the right and left levels of the **direction** factor. Responses were statistically different for rightward and leftward *extrapolated velocity* in the *Coherent 2D* ( $F(1,2) = 23.3$ ,  $* P = 0.04$ ) and *Coherent 2D'* ( $F(1,2) = 29.1$ ,  $* P = 0.03$ ) conditions only. In all the other conditions the responses were not statistically influenced by the side of the *extrapolated velocity* (*Coherent 3D*,  $F(1,2) = 0.03$ ,  $P = 0.87$ , *Incoherent 3D*,  $F(1,2) = 3.2$ ,  $P = 0.22$ , *Incoherent 2D*,  $F(1,2) = 0.32$ ,  $P = 0.63$ , *Incoherent 2D'*,  $F(1,2) = 1.6$ ,  $P = 0.33$ , *NoDotMotion*,  $F(1,2) = 0.38$ ,  $P = 0.6$ ). The main finding here is that, in contrast to what happened in the first experiment, subjects' responses did not indicate motion integration in the *Coherent 3D* condition.

Conditions were finally compared to each other with a Least Squares Difference Post-Hoc Test conducted on the difference between rightwards and leftwards scores: relatively to these differences, *Coherent 2D* and *2D'* conditions ( $** P < 0.001$ ) were statistically different from the *NoDotMotion* condition, confirming the integration effect for fronto-parallel translations. The *Co-*

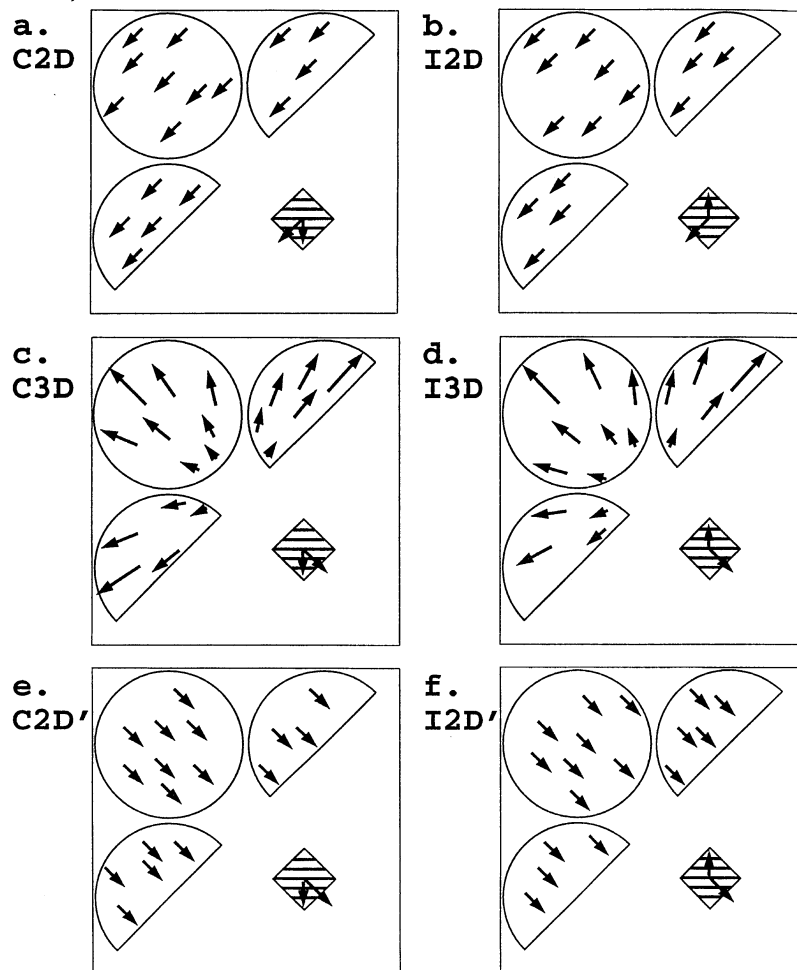


Fig. 6. Second experiment conditions. In these examples, for the *Coherent* conditions, the grating is moving downwards, while for the same dot velocity pattern, the grating is moving upwards in the *Incoherent* conditions. Compare to Fig. 3. In the seventh condition (*NoDotMotion*), the dots are stationary throughout stimulus presentation.

*herent 3D* and all *Incoherent* conditions (*2D*, *2D'* and *3D*) were not ( $P = 0.8$ ,  $P = 0.8$ ,  $P = 0.62$ , and  $P = 0.53$ , respectively). Again this shows that there is no 'repulsion' effect in the *Incoherent* conditions. *Coherent 2D* and *2D'* conditions were statistically different from their *Incoherent* counterpart (\*\*  $P < 0.001$ ), but were not statistically different from each other ( $P = 0.37$ ), indicating that there is no reliable difference between the two fronto-parallel translations. The *Coherent 3D* condition was not statistically different from the *Incoherent 3D* condition ( $P = 0.38$ ), confirming that there is no integration effect in *3D*. Finally, the *Coherent 3D* condition was statistically different from the *Coherent 2D* and *2D'* conditions (\*\*  $P < 0.005$  in both cases).

#### 4.1.2. Conclusions

In the two conditions of coherent fronto-parallel translation (*Coherent 2D* and *Coherent 2D'*), subjects perform in the same way as in experiment 1: their responses are compatible with the perception of a single

rigid object moving behind all apertures. This shows that the increase in distance between random dots and grating does not impair motion integration in these conditions. On the contrary, in the *Coherent 3D* condition subjects' answers are now similar to those in the *NoDotMotion* condition. This indicates that the missing dots were important in performing the task in the first experiment. In all *Incoherent* conditions subjects responded at chance level.

## 5. General discussion

### 5.1. Motion integration

Both experiments confirm previous results showing that the perceived movement of lines can be affected by moving dots. As compared to previous studies (Nakayama et al., 1988; Shiffrar et al., 1995) it is shown that this interaction can occur across space and beyond

the stationary contrast of the aperture outline. This study broadens these conclusions in two ways. First, such a spatial integration process can take place across distances that are rather large relative to the stimulus size (the dots do not have to lie in the vicinity of the ambiguously moving lines). In particular, it is found that such interactions can take place across  $5^\circ$  in central vision, for a size of the grating of  $2.3^\circ$ , for an exposure duration of 160 ms. Second, it was demonstrated that the spatial integration of velocity signals occurring across different apertures (such as has been demonstrated for lines by Lorenceau & Shiffrar, 1992) can also take place when the velocity field is not uniform,

but depicts translation in depth of a fronto-parallel plane.

## 5.2. Selection process

The results also clearly demonstrate that the coherence between the dot velocity pattern and the grating velocity is a prerequisite for the spatial integration process. Neither smoothing models based on a 2D or 3D constraint, nor global or local vector averaging can account for the difference between our *Coherent* and *Incoherent* conditions. Indeed, these models would predict that *Coherent* and *Incoherent* conditions elicits equal biases on the perceived direction of the grating. Rather, the bias was only observed in *Coherent* conditions, while *Incoherent* conditions elicited responses near chance level. This suggests that a selection step, based on the evaluation of motion consistency, is involved prior to the disambiguation of the grating velocity. Such a non-linear selection process seems also to be involved in transparency percepts, as illustrated with plaids by van den Berg and van de Grind (1993).

In Section 2, ‘Coherent’ and ‘Incoherent’ conditions are defined on the basis of the consistency of the *extrapolated velocity* with the grating constraint line. Clearly, the results of the first experiment are compatible with a selection process based on the comparison between the *extrapolated velocity* and the grating constraint line. In the following one examines whether other selection criteria can account for the perceptual differences between *Coherent* and *Incoherent* conditions in both experiments.

## 5.3. Individual dots

In 2D conditions each individual dot defines the same constraint point in 2D velocity space. This constraint is consistent with the grating constraint line in the *Coherent* conditions and inconsistent in the *Incoherent* conditions (Fig. 8a). Thus, in these conditions, the results are compatible with a selection process based on the constraint consistency between any dot and the grating.

In 3D conditions, each dot defines a specific constraint point that is distinct from the others. Only a small fraction of dot velocities are consistent with the grating constraint line (Fig. 8b): in the *Incoherent 3D* condition the consistent dot constraints are symmetrically distributed on the right and left side of the grating constraint line, while in the *Coherent 3D* condition, they all lie on the side opposite to the *extrapolated velocity*. Therefore, an integration process based on the distribution of consistent dot constraints would predict chance level in the *Incoherent 3D* condition, which was observed, and an inversion of rightwards versus leftwards responses in the *Coherent 3D* condition. Such an inversion of the response pattern was never observed in

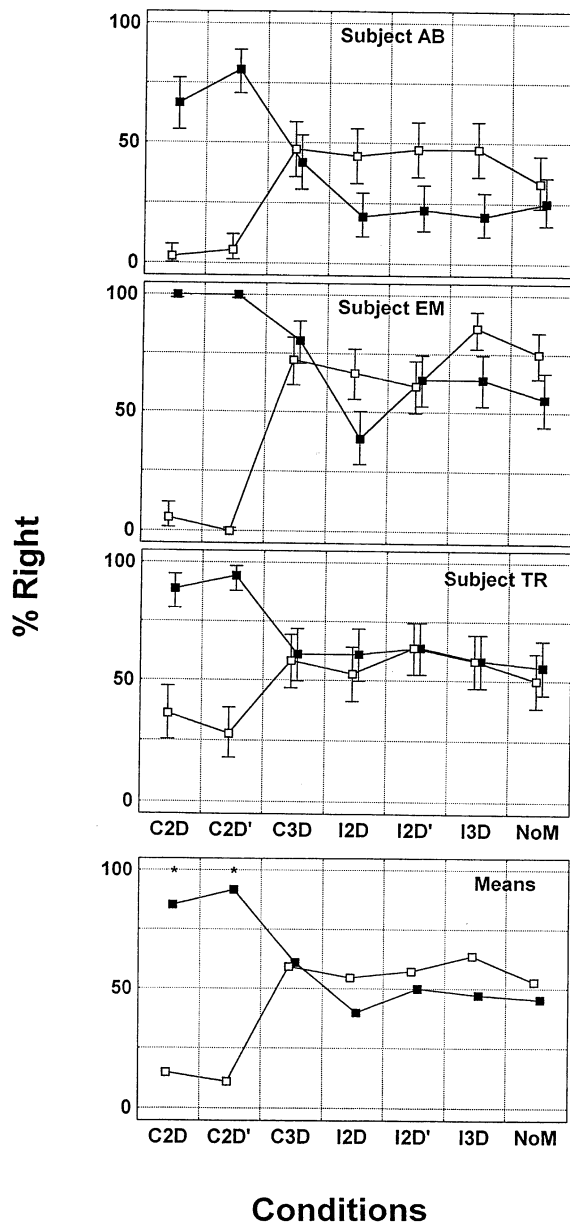


Fig. 7. Results of the second experiment in the seven conditions for the three subjects. Responses are averaged over all grating positions. See Fig. 4.

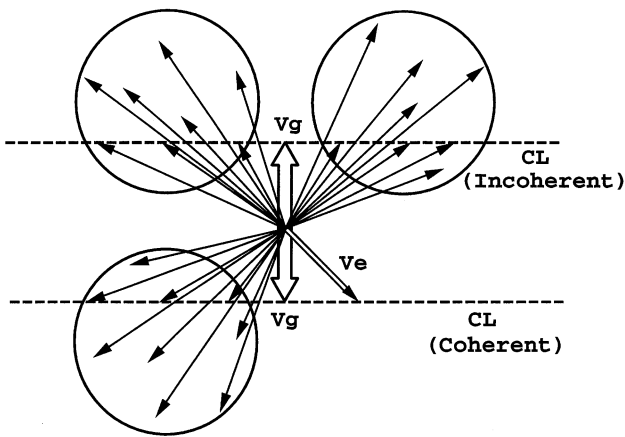


Fig. 8. Velocity space representation of the expansion velocity field for 3D conditions in the first experiment. The velocities of dots belonging to the same circular aperture define a circular area.  $V_g$ : grating velocity; CL: grating constraint line;  $V_e$ : extrapolated velocity. For the uniform flow field, the dot velocity and extrapolated velocity are identical.

this condition, neither in the first nor in the second experiment. Hence the selection process is seemingly not based on the analysis of consistency between individual dot constraints and the grating constraint, rejecting approaches that rely on the clustering of IOC in 2D velocity space, even if it is performed on local patches as proposed by Schunck (1986).

#### 5.4. Three-dimensional velocity field hypothesis

The third conclusion is that the scheme proposed by Droulez and Cornilleau-Pérès (1993) involving the smoothness of the 3D velocity field, or models that use a parametric representation of the optic flow (e.g. affine, Bouthemy & Santillana-Rivero, 1987) are seriously questioned. The second experiment showed that the *extrapolated velocity* is not used by the selection process to disambiguate the grating velocity, casting doubts on any mechanism that would correctly extrapolate the dot motion pattern at the locus of the grating (e.g. 3D motion computation or affine representation of the velocity field). However, the modification of the aperture geometry changed the stimuli in several ways: a decrease in the total number of visible dots, in the total area of the apertures and an increase in the distance between the lines and their nearest dots. Droulez and Cornilleau-Pérès (1993) pointed out that the computation of the third component (the velocity-in-depth) of the 3D velocity field is more sensitive to noise and converges more slowly. Thus this component would be more sensitive to the modifications of the stimulus, and the integration mechanism would be more sensitive in the 3D conditions than in the 2D conditions. It cannot be excluded that the discrepancy between the first and second experiment results reflects

such sensitivity. Moreover 3D integration could require longer exposure to the moving stimuli, as compared to 2D integration. Longer stimulus durations may therefore make 3D integration easier.

#### 5.5. Local velocity averaging

In the *Coherent 3D* conditions the modification of the aperture geometry resulted in a dramatic change of subject responses. As noted above, the integration process might be more sensitive to the stimulus parameters in 3D conditions than in 2D conditions. However, the stimulus manipulations were primarily done to modify its 2D velocity content, in such a way that no local averaging of dot 2D velocities could be correlated with the *extrapolated velocity*. One now examines whether such an explanation based on a local averaging scheme in 2D velocity space might explain all the data. It is shown that a selection process based on motion extrapolation through local velocity averaging could indeed account for the results in all conditions of both experiments.<sup>2</sup>

The local mean velocity (LMV) was calculated as the average of individual dot 2D velocities over a circular region of radius  $R$ , centered on the grating. For 2D translations any averaging of dot velocities confounded with the velocity of each dot, and the discussion of motion consistency for averaged velocities then amounts to the above considerations concerning single dot constraints. In order to account for 2D conditions, the size of the averaging field must be sufficient to encompass at least one dot in the second experiment (i.e. the radius must be superior to  $5^\circ$ ).

In Fig. 9, the vertical component of LMV for the expansion velocity field is plotted as a function of  $R$ . It is to be compared to the vertical component of grating velocity (dotted lines), which defines the grating constraint line. Because of the symmetry of the velocity field, the horizontal and vertical components of the LMV are equal. In the first experiment the LMV for small radii almost coincides with the *extrapolated velocity*. Hence it lies close to the grating constraint line in the *Coherent 3D* condition and could account for subjects' high scores on this condition. In all other 3D conditions, the LMV is not compatible with the grating constraint line, which could explain the chance level responses actually given by the subjects. With large radii the LMV is always in the direction opposite to the

<sup>2</sup> As one reviewer pointed out, interpolation of the dot velocities at the position of the grating was possible in the first but not in the second experiment. It is therefore possible to account for our results in the 3D conditions with a scheme based on interpolation rather than extrapolation. This, however, would implicate that motion integration is based on a different mechanism in the case of uniform motion.

## First Experiment

## Second Experiment

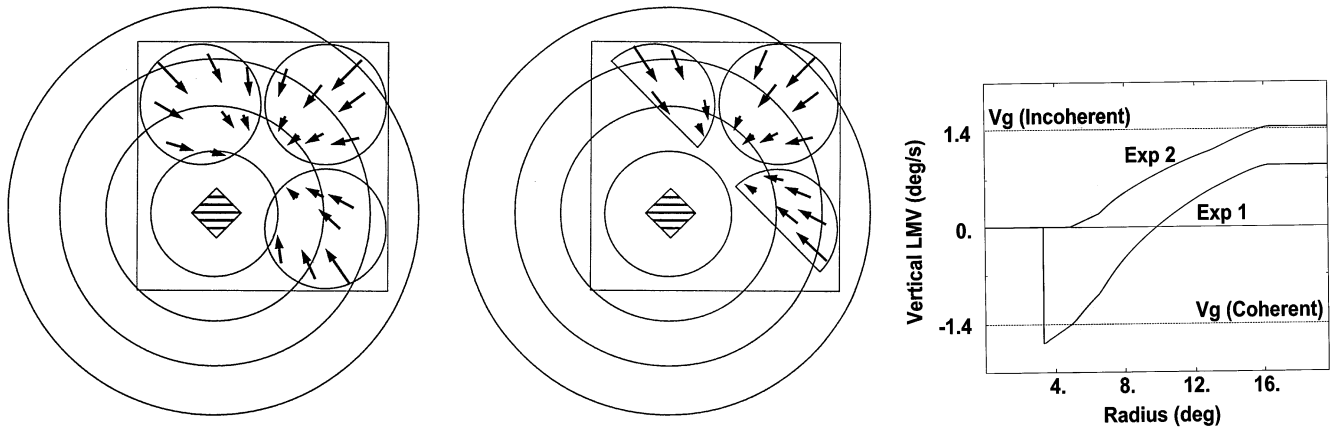


Fig. 9. Computation of local mean velocity (LMV) from 2D spatial integration. (a) The integration area is centered on the grating. Several integration areas with different radii are shown superimposed to the velocity field for the two experiments. (b) Vertical component of mean dot velocity as a function of the radius of the circular integration area, for first and second experiment 3D conditions. Vg: grating velocity (in the coherent case it is equal to the vertical component of the *extrapolated velocity*).

*extrapolated velocity*. It is therefore consistent with the grating line constraint in the *Incoherent 3D* conditions, which would predict 'repulsion' effects in these conditions and no effects in the *Coherent* conditions. With intermediate radii, the predictions depends on the accuracy of the selection process: if this mechanism tolerates some discrepancy between the LMV and the constraint line, for radii between 8 and 10° the prediction is integration in the first experiment *Coherent 3D* condition, and 'repulsion' in the second experiment *Incoherent 3D* condition. The radii compatible with all our results ranges therefore between 5 and 8° of visual angle.

Although the LMV hypothesis can explain the data, it is important to note that our stimuli were not designed specifically to test it. Its sole purpose here is to show that one can find parameters that render such a scheme compatible not only with the *Coherent 3D* conditions, but with all the conditions used, in both experiments. Moreover it is only a crude example of the kind of local mechanisms that could be used to define a selection criterion compatible with the results. Other local integration schemes (e.g. weighted sum, as in the motion coherence theory of Yuille & Grzywacz, 1988) would certainly do as well, as soon as they naturally embed spatial interactions within a limited area.

## 6. Conclusion

It has been demonstrated that the perceived direction of a moving grating can be influenced by a moving random dot pattern, for uniform and non-uniform velocity fields. Moreover, this integration step is preceded

by the evaluation of the consistency between the grating constraint line and the dot motion pattern: the perceived direction of the grating is strongly influenced only when the movements of dots and lines are compatible with a single rigid motion.

When the grating is captured, its perceived direction is compatible with the rigid motion of the dot pattern, even though in the case of non-uniform velocity field none of the dots in the stimulus indicates this direction in 2D velocity space. Therefore the experiments enable one to reject schemes based on the analysis of consistency between individual motion signals and the grating constraint in 2D velocity space. However, for non-uniform velocity fields the capture of the grating is weaker than for fronto-parallel translations and can be disrupted by manipulating the geometry of the apertures. Whether the effect of aperture manipulation is due to the increase in distance between dots and lines or to the change in the dot velocity distribution remains unresolved and other experiments would be needed to characterize the type of signals used by the integration process.

Finally the results are consistent with the common decomposition of motion processing in several steps, but emphasize the need to go beyond the simple uniform motion in the study of motion integration and segmentation.

## References

- Adelson, E. H., & Bergen, J. R. (1985). Spatiotemporal energy models for the perception of motion. *Journal of the Optical Society of America (A)*, 2, 284–298.

- Adelson, E. H., & Movshon, J. A. (1982). Phenomenal coherence of moving visual patterns. *Nature*, *300*, 523–525.
- van den Berg, A. V., & van de Grind, W. A. (1993). Do component motion recombine into a moving plaid percept? *Experimental Brain Research*, *93*, 312–323.
- Bouthemy, P. and Santillana-Rivero, J. (1987). A Hierarchical likelihood approach for region segmentation according to motion-based criteria. *Proceedings of the First IEEE International Conference on Computer Vision*, 463–467.
- Burke, D., & Wenderoth, P. (1993). The effect of interactions between one-dimensional component gratings on two-dimensional motion perception. *Vision Research*, *33*, 343–350.
- Droulez, J., & Cornilleau-Péres, V. (1993). Application of the coherence scheme to the multisensory fusion problem. In A. Berthoz, *Multisensory control of movement* (pp. 485–501). Oxford: Oxford University Press.
- Duffy, C. J., & Wurtz, R. H. (1991a). Sensitivity of MST neurons to optic flow stimuli. I. A continuum of response selectivity to large-field stimuli. *Journal of Neurophysiology*, *65*, 1329–1345.
- Duffy, C. J., & Wurtz, R. H. (1991b). Sensitivity of MST neurons to optic flow stimuli. II. Mechanism of response selectivity revealed by small field stimuli. *Journal of Neurophysiology*, *65*, 1346–1359.
- Felleman, D. J., & Van Essen, D. C. (1991). Distributed hierarchical processing in the primate visual cortex. *Cerebral Cortex*, *1*, 1–47.
- Gorea, A., & Lorenceau, J. (1991). Directional performances with moving plaids: component-related and plaid-related processing coexist. *Spatial Vision*, *5*, 231–252.
- Hildreth, E. C. (1984). The computation of the velocity field. *Proceedings of the Royal Society of London B*, *221*, 189–220.
- Horn, B. K. P., & Schunck, B. G. (1981). Determining optical flow. *Artificial Intelligence*, *17*, 185–203.
- Hubel, D., & Wiesel, T. (1968). Receptive fields and functional architecture of the monkey visual cortex. *Journal of Physiology*, *195*, 215–243.
- Koenderink, J. J., & van Doorn, A. J. (1987). Facts on optic flow. *Biological Cybernetics*, *56*, 247–254.
- Kooi, F. L., De Valois, K. K., Grosf, D. H., & De Valois, R. L. (1992). Properties of the recombination of one-dimensional motion signal into a pattern motion signal. *Perception and Psychophysics*, *52*, 415–424.
- Lagae, L., Maes, H., Raiguel, S., Xiao, D.-K., & Orban, G. A. (1994). Responses of macaque STS neurons to optic flow components: a comparison of areas MT and MST. *Journal of Neurophysiology*, *71*, 1597–1626.
- Lamouret, I., Cornilleau-Péres, V., & Droulez, J. (1995). Solving the aperture problem in a three-dimensional context. *Perception (Supplement)*, *24*, 103.
- Longuet-Higgins, H. C., & Prazdny, K. (1980). The interpretation of moving retinal images. *Proceedings of the Royal Society of London B*, *208*, 385–397.
- Lorenceau, J., & Shiffrar, M. (1992). The influence of terminators on motion integration across space. *Vision Research*, *32*, 263–273.
- Marr, D. (1982). *Vision*. San Francisco, CA: Freeman.
- Marr, D., & Ullman, S. (1981). Directional selectivity and its use in early visual processing. *Proceedings of the Royal Society of London B*, *211*, 151–180.
- Maunsell, J. R. H., & Van Essen, D. C. (1983). The connections of the middle temporal visual area (MT) and their relationship to a cortical hierarchy in the macaque monkey. *Journal of Neuroscience*, *3*, 2563–2586.
- Mingolla, E., Todd, J. T., & Norman, J. F. (1992). The perception of globally coherent motion. *Vision Research*, *32*, 1015–1031.
- Movshon, J. A., Adelson, E. H., Gizzi, M. S., & Newsome, W. T. (1985). The analysis of moving visual patterns. In C. Chagas, et al., *Pattern recognition mechanisms* (pp. 117–151). Berlin: Springer-Verlag.
- Nakayama, K., & Silverman, G. H. (1988). The aperture problem — I. Perception of nonrigidity and motion direction in translating sinusoidal lines. *Vision Research*, *28*, 739–746.
- Nowlan, S. J., & Sejnowski, T. J. (1995). A selection model for motion processing in area MT of the primate. *The Journal of Neuroscience*, *15*, 1195–1214.
- Perrone, J. A., & Stone, L. S. (1994). A model of self-motion estimation within primate extrastriate visual cortex. *Vision Research*, *34*, 2917–2938.
- Saito, H., Yukie, M., Tanaka, K., Hikosaka, K., Fukuda, Y., & Iwai, E. (1986). Integration of direction signals of image motion in the superior temporal sulcus of the macaque monkey. *Journal of Neuroscience*, *6*, 145–157.
- Schunck, B. G. (1986). Image flow segmentation and estimation by constraint line clustering. *IEEE Transactions on PAMI*, *11*, 1010–1027.
- Scott, G.L. (1986). Smoothing the optic flow field under perspective projection. *Proceedings of the IEEE Conference on Computer Vision and Pattern Recognition*, 504–509.
- Shiffrar, M., Li, X., & Lorenceau, J. (1995). Motion integration across differing image features. *Vision Research*, *15*, 2137–2141.
- Snedecor, G. W., & Cochran, W. G. (1989). *Statistical methods* (8th edition, pp. 289–290). Ames, Iowa: Iowa State University Press.
- Stone, L. S., Watson, A. B., & Mulligan, J. B. (1990). Effect of contrast on the perceived direction of a moving plaid. *Vision Research*, *30*, 1049–1067.
- Tanaka, K., Sugita, Y., Moriya, M., & Saito, H. (1993). Analysis of object motion in the ventral part of the medial superior temporal area of macaque visual cortex. *Journal of Neurophysiology*, *69*, 128–142.
- Tziritas, G. (1987). Estimation of motion and structure of 3-D objects from a sequence of images. *Proceedings of the First IEEE International Conference on Computer Vision*, 693–697.
- Van Santen, J. P. H., & Sperling, G. (1984). Temporal covariance model of human motion perception. *Journal of the Optical Society of America*, *A1*, 451–473.
- Wallach, H. (1935). Über visuell wahrgenommene Bewegungsrichtung. *Psychologische Forschung*, *20*, 325–380. English translation in Wuerger, S., Shapley, R. and Rubin, N. (1996). ‘On the visually perceived direction of motion’ by Hans Wallach: 60 years later. *Perception*, *25*, 1317–1367.
- Wallach, H. (1976). On perceived identity: I. The direction of motion of straight lines. In H. Wallach, *On perception* (pp. 201–216). New York: Quadrangle, The New York Times Books Co.
- Wilson, H. R., Ferrera, V. P., & Yo, C. (1992). A psychophysically motivated model for two dimensional motion perception. *Visual Neuroscience*, *9*, 79–97.
- Yo, C., & Wilson, H. R. (1992). Perceived direction of moving two-dimensional patterns depends on duration, contrast and eccentricity. *Vision Research*, *32*, 135–147.
- Yuille, A. L., & Grzywacz, N. M. (1988). A computational theory for the perception of coherent visual motion. *Nature*, *333*, 71–74.